

On the 3D printing of recycled ABS, PLA and HIPS thermoplastics for structural applications

ABS, PLA and
HIPS
thermoplastics

Ranvijay Kumar and Rupinder Singh

*Department of Production Engineering, Guru Nanak Dev Engineering College,
Ludhiana, India, and*

Ilenia Farina

Department of Engineering, University of Naples, Naples, Italy

115

Received 10 July 2018
Revised 28 July 2018
Accepted 28 July 2018

Abstract

Purpose – Three-dimensional printing (3DP) is an established process to print structural parts of metals, ceramic and polymers. Further, multi-material 3DP has the potentials to be a milestone in rapid manufacturing (RM), customized design and structural applications. Being compatible as functionally graded materials in a single structural form, multi-material-based 3D printed parts can be applied in structural applications to get the benefit of modified properties.

Design/methodology/approach – The fused deposition modelling (FDM) is one of the established low cost 3DP techniques which can be used for printing functional/ non-functional prototypes in civil engineering applications.

Findings – The present study is focused on multi-material printing of primary recycled acrylonitrile butadiene styrene (ABS), polylactic acid (PLA) and high impact polystyrene (HIPS) in composite form. Thermal (glass transition temperature and heat capacity) and mechanical properties (break load, break strength, break elongation, percentage elongation at break and Young's modulus) have been analysed to observe the behaviour of multi-material composites prepared by 3DP. This study also highlights the process parameters optimization of FDM supported with photomicrographs.

Originality/value – The present study is focused on multi-material printing of primary recycled ABS, PLA and HIPS in composite form.

Keywords FDM, Multi-material printing, ABS, Mechanical properties, Thermal

Paper type Research paper

© Ranvijay Kumar, Rupinder Singh and Ilenia Farina. Published in *PSU Research Review*. Published by Emerald Publishing Limited. This article is published under the Creative Commons Attribution (CC BY 4.0) licence. Anyone may reproduce, distribute, translate and create derivative works of this article (for both commercial and non-commercial purposes), subject to full attribution to the original publication and authors. The full terms of this licence may be seen at <http://creativecommons.org/licenses/by/4.0/legalcode>

The authors are highly thankful to Mr. Paramvir Singh (M Tech scholar), Mr. Kshitij Bhatia, Mr. Manshant Singh and Mr. Himmatpal Singh (U.G Students) for their sincere efforts. Authors are also thankful of manufacturing research lab (GNDEC, Ludhiana) for providing financial/technical assistance to carry out the research work.

IF acknowledges financial support from the Department of Engineering, University of Naples Parthenope.



1. Introduction

The three-dimensional printing (3DP) is known as 'additive manufacturing' which forms the object by successive layers of materials for different application areas (Singh *et al.*, 2018b; Singh *et al.*, 2018d). It has the potential/impact to transform manufacturing supply chain, distribution channel and business model (Kumar *et al.*, 2018). But when fabricated components are evaluated on the basis of mechanical durability, 3DP is seen as the doubtful techniques and, therefore, a challenge to the researchers and scientist is to improve the mechanical/thermal properties of the parts prepared. There are many commercially available 3DP technologies (Singh *et al.*, 2018b; Singh *et al.*, 2018d; Kumar *et al.*, 2018; Kumar *et al.*, 2017a; Kumar *et al.*, 2017b; Singh *et al.*, 2016) like fused deposition modelling (FDM), stereo lithography (SLA), inkjet printing, selective laser sintering (SLS), digital light manufacturing (DLP), selective laser melting (SLM), electronic beam melting (EBM), laminated object manufacturing (LOM), etc. The FDM is the melt extrusion process in which robotic device works on the CNC/NC programming to control the heating and movement of the filaments. The extruded material through the nozzle head is directed on the print bed and immediately hardened to ensure the part fabrication. To ensure the better dimensional stability of the component formed, it is required to process the printing below the melting point of the substrate (Kariz *et al.*, 2018; Hambali *et al.*, 2017). The sustainability of the part produced by the FDM is the function of the filament preparation (extrusion is the basic process used for the preparation of feedstock filaments). The extrusion process is increasingly important from sustainability viewpoints for targeting reusability of waste thermoplastic materials (Singh *et al.*, 2018c). Mechanical properties of FDM fabricated parts are highly dominated by their filament processing. The mechanical sustainability of the fabricated part is dependent upon the nature of processing of the initial component (grinding, extrusion, etc.), barrel temperature, rotational speed and torque are some of the input variable during the filament processing which largely affects the mechanical sustainability of the FDM fabricated parts (Singh and Singh, 2016).

Manufacturing and technology environments are fuelling a new generation of engineer, scientist and designers. Just as it made at home polymer 3D printers a commonality today, the world could eventually see a metal or ceramic 3D printer become common in an average household. To achieve this goal, future inventions in next generation structures using existing materials via AM will surely need to revolve around cost reduction, improved performance and advanced structural design (Bandyopadhyay and Heer, 2018). The study conducted for 3DP of multilateral component of acrylonitrile butadiene styrene (ABS) and thermoplastic polyurethane (TPU) reveals with support of 3D imaging that interface properties are found in control with good layers connectivity (Guessasma *et al.*, 2017). Multi-material 3DP has the potentials to be a milestone in RM, customized design and structural applications. Being compatible of functionally graded materials in a single structural form it can be applied potentially in structural application to get the benefit of combined properties of different materials. The multi-material printing provides a fast and robust structure with compact functionality of all combined materials (Muguruza *et al.*, 2017; Ngo *et al.*, 2018). It was suggested that hybrid manufacturing (additive + subtractive) process can fulfil the demand of high dimensional accuracy, less post-processing with improved surface properties (Lee *et al.*, 2017). The multi-material 3DP has fascinating applications for new smart 4D structures which can provide the achievement of shape/property/functionality (Momeni *et al.*, 2017). It was highlighted that existing AM techniques such as FDM can be modified to hybrid deposition manufacturing (HDM) with embedded component to produce more complex, integrated multi-material component than traditional techniques (Ma *et al.*, 2015). It was reported that build orientation, fabrication parameters and associated variable can largely affect the connection between the multilateral interfaces during 3D printing, so this should be optimized to get better

mechanical, thermal and surface properties (Bittner *et al.*, 2018; Meisel, 2015; Mohammed *et al.*, 2016; Vu *et al.*, 2018). ABS is common thermoplastic which is amorphous in nature and having high impact resistance, low thermal conductivity, heat resistance and toughness to potentially applicable in civil engineering field. Generally, two types of ABS are classified one as ABS for moulding and other as ABS for extrusion/printing. The impact and toughness strength of ABS can be amplified by increasing the proportion of polybutadiene in relation with styrene and acrylonitrile in ABS matrix (Rutkowski and Levin, 1986). Polylactic acid (PLA) is a biodegradable and bioactive thermoplastic material derived from renewable resources such as corn starch, cassava roots, chips or sugarcane. The PLA exhibits the range of crystallinity and mechanical properties in between the polystyrene and polyethylene terephthalate. The biodegradability and bio-compatibilities are the key advantages of PLA to promote its use in the structural and bio-medical applications (Martin and Averous, 2001). 'High impact polystyrene' (HIPS) is a low-cost polymer which provides the ease of fabrication and machining. It is categorized as the low strength structural application when it is required to have low cost impact strength, machinability and fabrication. It is largely used for the pre-production prototypes since it has high dimensional stability and ease to fabrication, paint and glue. ABS, PLA and HIPS are differently characterized thermoplastic material, which allow the FDM processes for fabrication of advanced graded component with superior functionality at different scales (Kumar and Singh, 2018; Singh *et al.*, 2017b; Singh *et al.*, 2018a; Singh *et al.*, 2017c; Singh and Kumar, 2017; Singh *et al.*, 2017d; Barretta *et al.*, 2017).

The literature survey reveals that multi-material component comprised of advantages of all the material combined together and can be potentially applied in the area of civil engineering fields especially in structural application. As FDM is the cost-effective technique, this can be a potential tool for fabrication of multi-material component at minimum cost. In the present study, differently characterized ABS, PLA and HIPS were selected as multi-material and 3D printed together to combine the advantages of all polymers. Thermal (Heat capacity at glass transition temperature, thermal conductivity) and mechanical (break elongation, break load, percentage elongation at break, break strength and Young's modulus in tensile as well as pull out test) properties have been investigated of 3D printed multi-material component.

2. Materials and methods

Three different thermoplastics (namely: ABS, PLA and HIPS) were selected for the experimentation. ABS is amorphous in nature and having high impact resistance. Low thermal conductivity, heat resistance and toughness, bio-degradability and bio-compatibilities are the key advantages of PLA, whereas HIPS is a low strength structural polymer which have better machinability and fabrication characteristics with low cost. During pilot study, all three selected thermoplastic were subjected to thermal and mechanical testing, which resulted in dissimilar mechanical/thermal properties as anticipated. PLA was observed with maximum break elongation, break load, break strength, heat capacity rate and melt flow index (MFI) but minimum Young's modulus and glass transition temperature, whereas HIPS was observed just opposite of PLA (Table I). So, detailed study was conducted to combine these materials in a single form so that final product may have the advantages of all thermoplastics. The break load, break strength and Young's modulus are the properties which are desired to be in maximum, whereas break elongation and percentage elongation at break are properties which desired to be minimum for structural engineering application.

The twin screw extrusion (TSE) was used to prepare the feedstock filaments of diameter 1.75 ± 0.05 mm. The file format of .STL was sliced in 12 layers of 0.27 mm layer thickness, it

was sliced to form the 4 layers each of ABS, PLA and ABS. Followed by preparations of experimental design multi-material 3D printed components based upon ASTM D638 type IV have been prepared and then tested for tensile properties. Multifactor optimization based upon analysis of variance (ANOVA) has been conducted on mechanical properties (along with testing of thermal conductivity and flexural properties at optimized conditions). The detailed step by step procedure is shown in Figure 1.

3. Experimentation

The experimentation phases of present study include systematic practices of MFI characterization, differential scanning calorimetric (DSC) analysis, extrusion of feedstock filaments, 3D printing on FDM setup and mechanical testing for properties evaluation.

3.1 MFI characterization

MFI is one of the rheological properties which determine the flow ability of material. Sometimes MFI can be most important consideration because it can determine the viscosity, hardness, shear strength and other mechanical-thermal characteristics of the product at an elevated temperature. ASTM D1238 standard in the present study was used at 230°C with applicable weight of 3.8Kg for ABS, PLA and HIPS for MFI evaluation with material collected through the nozzle in gm/10minute. Figure 2 shows 3D view of MFI indexer.

3.2 DSC

DSC is analytical tool for determination of thermal properties including melting points, glass transition temperature, solidification temperature, degree of crystallinity, heat capacity rate,

Table I.
Mechanical, thermal and rheological properties of ABS, PLA and HIPS

Polymer	Break elongation (mm)	Elongation at break (%)	Break load (N)	Break strength (MPa)	MFI (g/10 min)	Glass transition temp (°C)	Young's modulus (MPa)	Heat capacity rate (J/g)
ABS	4.94	7	186.3	9.7	8.76	109.76	175	1.36
PLA	5.13	7	254.16	13.24	13.52	62.57	47.9	1.47
HIPS	2.47	3	72.72	3.79	7.50	100.41	112.5	1.17

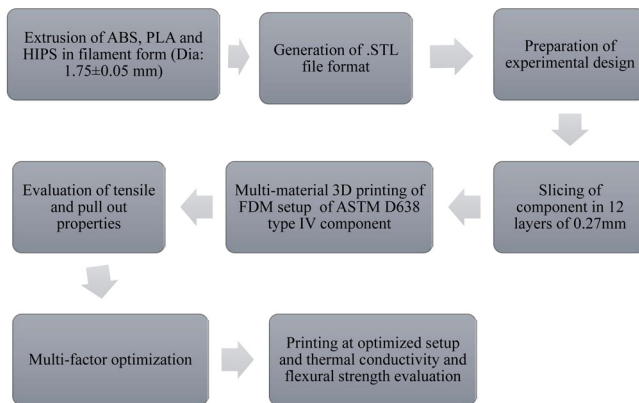


Figure 1.
Steps involved in multi-material 3D printing

etc. These properties are defined under the controlled continuous heating (endothermic reaction) and controlled continuous cooling (exothermic reaction). The endothermic reaction was carried under the heating rate of $+10^{\circ}\text{C}/\text{min}$ from 30°C to 250°C , whereas exothermic reaction was carried under $-10^{\circ}\text{C}/\text{min}$ from 250°C to 30°C . Figure 3 show the experimental setup of a DSC and internal configurations.

ABS, PLA and
HIPS
thermoplastics

3.3 TSE

Extrusion is the process for preparation of feedstock in continuous form. There are variety of the continuous extruder available which are classified based on the nature of operation, intermeshing, axis of rotation and rotation direction. Extrudes are broadly divided in single screw extruder (SSE), TSE. Figure 4 shows the detailed classification of screw extrusion process. For the present study, TSE with intermeshing with co-rotating screws has been used to form feedstock polymeric composite. In the present case, extrusion with TSE was

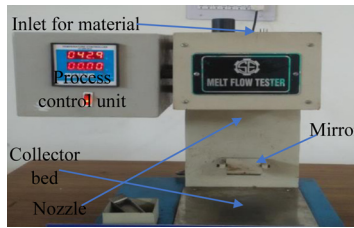


Figure 2. Schematic configuration of MFI indexer

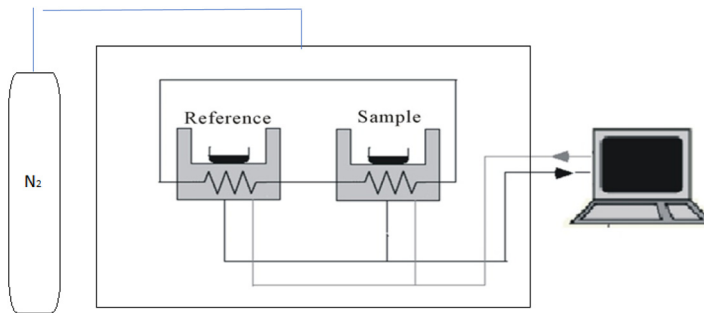


Figure 3. Schematic of DSC

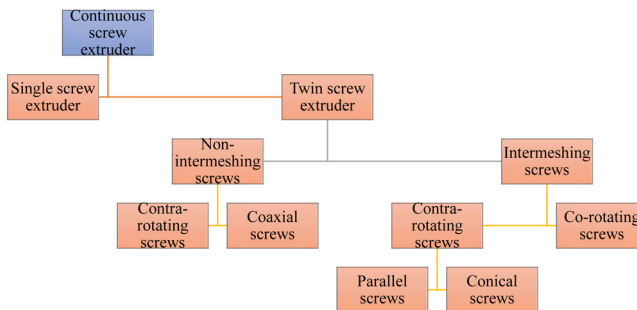


Figure 4. Classification of extrusion process

performed under the temperature of 230°C, rotational speed of 50 rpm and with applied load of 10 Kg to prepare the feedstock filaments of 1.75 ± 0.05 mm. The extrusion parameters were determined by pilot experimentation based on uniformity and dimensional accuracy. Figure 5 shows the 3D view of TSE used in present study.

3.4 FDM

Commercial open source FDM setup (Company: Divide by Zero) configured with two nozzle head was selected for multi-material 3D printing. The static parameters for fabrication of composite parts were include nozzle diameter of 0.3 mm, filament diameter of 1.75 ± 0.05 mm, layer height 0.27 mm, 3 perimeters (by adjusting 3 top and 3 bottom layers), rectilinear fill pattern, 30 mm/sec perimeter speed, travel speed of 130 mm/sec, at extrusion temperature of 250°C and bed temperature of 55°C. The two parameters were varied for fabrication of part on FDM (i) infill percentage of 60, 80 and 100 per cent, (ii) printing speed of 50, 60 and 70 mm/sec. The multi-material printing was customized by total 12 layers with 4 layers of each material. The multi-material printing was configured as APH (four layers of ABS on bottom, four layers of PLA in middle and four layers of HIPS on top), PHA (four layers of PLA on bottom, four layers of HIPS in middle and four layers of ABS on top) and HAP (four layers of HIPS on bottom, four layers of ABS in middle and four layers of PLA on top). The design of experiment based upon Taguchi L9 orthogonal array has been prepared and fabrication of component was performed by following design sheet (Table II).

The 3D printing of multi-material on FDM was processed by following systematic steps. First, design of tensile component of dimension as per ASTM D 1238 type IV has been prepared on SOLIDWORKS software and converted to the file type .STL. The prepared file

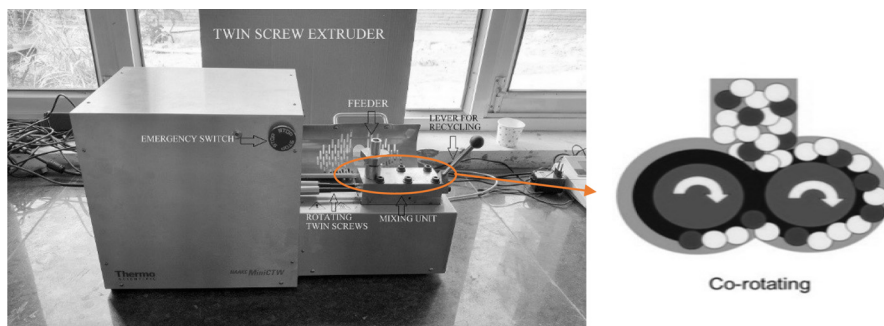


Figure 5. Photographic view of the experimental setup for extrusion of feedstock filaments

Table II. Design of experiment of multi-material 3D printing

Experiment no.	Material combination	Infill (%)	Printing speed (mm/sec)
1	APH	60	50
2	APH	50	60
3	APH	100	70
4	PHA	60	60
5	PHA	80	70
6	PHA	100	50
7	HAP	60	70
8	HAP	80	50
9	HAP	100	60

of .STL file format was fed to the KISSLICER software to slice the designed component. A total of 12 layers of 0.27 mm layer thickness has been sliced by varying the infill percentage of 60, 80 and 100 per cent under printing speed of 50, 60 and 70 mm/sec as per [Table II](#). After this, an adhesion media of ABS + acetone was prepared by stirring it in ultrasonic stirrer for 30 min. The adhesion solvent was dispersed on the FDM bed and allowed to get dry for 5 min as standard for all. Then printing command has been given to fabricate the functional prototypes of ASTM D 638 type IV. [Figure 6](#) shows the commercial FDM setup and printing of functional prototypes. [Figure 7](#) shows functional prototypes of composites (ABS+PLA+HIPS) printed as per [Table II](#).

3.5 Tensile testing

Tensile testing of 3D printed multi-material component was performed on universal testing machine (UTM) under room temperature of 28°C and tensile speed of 20mm/min as a standard for all components. The output of tensile testing has been selected as break elongation, percentage elongation at break, break load, break strength and Young's

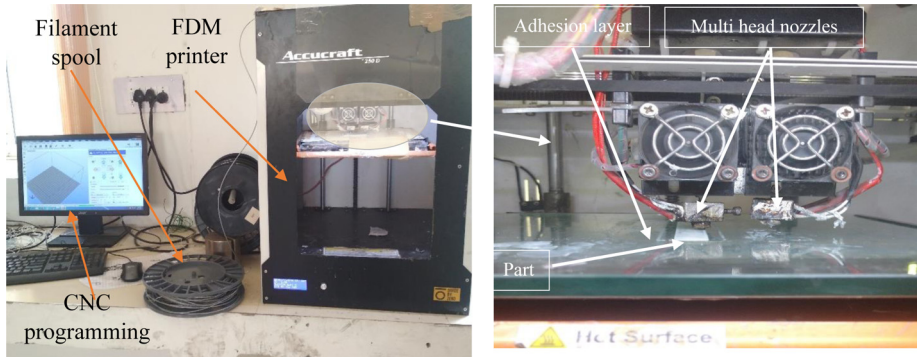


Figure 6.
Commercial FDM
setup



Figure 7.
3D printed multi-
material component
as per ASTM D 638
type IV

modulus. Figure 8 shows the experimental setup for tensile properties evaluation and fracture parts after testing.

3.6 Lee's disc thermal conductivity measurement

The Lee's disc method of thermal conductivity measurement is applicable to all the poorly conducting materials like: woods, polymer, non-metals, glass and fibres. The method of thermal conductivity measurement by this method was first reported by the British scientist Lee. The Lee's disc method is one of the established methods of thermal conductivity measurement techniques which results a reliable output. Figure 9 shows the experimental setup of Lee's disc apparatus for thermal conductivity measurement.

The FDM was used to fabricate the component of diameter 110mm and thickness (x) of 3.3 mm. This functional dimension has been used to check its thermal conductivity by Lee's disc method. The samples of ABS, PLA and HIPS were printed separately and as multi material followed by its thermal conductivity evaluation. Following heat flow equation has been used for calculating thermal conductivity:

$$K = \frac{M.S.\left(\frac{dt}{dT}\right).x}{A.(t_1 - t_2)} \tag{1}$$

where K is the thermal conductivity, M is the mass of metallic disc = 0.769Kg, S is the specific heat capacity of Lee's disc = 377 J/Kg-K, dt/dT is temperature gradient, A is the area of sample = 0.0095 m², t₁ is the steady temperature of steam chamber = 367K and t₂ is the steady temperature of the Lee's disc = 337K.



Figure 8.
Experimental view of UTM and fractured parts by tensile testing

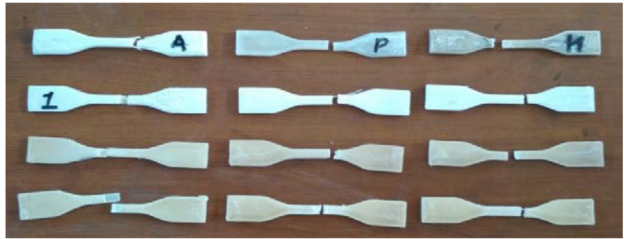


Figure 9.
Thermal conductivity measurement by Lee's disc theory

Here, the temperature gradient (dt/dT) of ABS, PLA and HIPS were observed as:

$$\text{ABS} = 0.0513 \text{ K/s, PLA} = 0.0663 \text{ K/s and HIPS} = 0.0963 \text{ K/s.}$$

Them upon putting the values of dt/dT of ABS, PLA and HIPS in [Equation \(1\)](#) given as:

$$K_{\text{ABS}} = 0.1722 \text{ W/m.K.}$$

$$K_{\text{PLA}} = 0.2225 \text{ W/m.K.}$$

$$K_{\text{HIPS}} = 0.3232 \text{ W/m.K.}$$

3.7 Flexural testing (three-point bend test)

The flexural strength is one of the most important consideration of the component to be applied in engineering applications. The flexural test at optimized processing variables has been performed as per ASTM D7264/D7264M – 15. [Figure 10](#) shows the setup of flexural test and tested component.

3.8 Pull out testing

For structural engineering application of 3D printed multi-material component, it must fulfil the qualification on the basis of pull out properties. The comparative analysis of all nine samples has been conducted under the pull speed of 5 mm/min. The pull-out testing resulted in calculation of break load, break strength, break elongation and percentage elongation at break to check the capabilities of 3D printed multi-material component.

4. Results and discussion

The samples of recycled ABS, PLA and HIPS thermoplastic were subjected to thermal and mechanical testing. The PLA was observed with maximum break elongation, break load, break strength, heat capacity rate and melt flow index (MFI) but minimum Young's

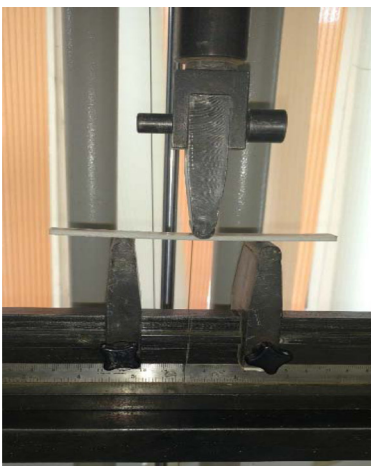


Figure 10.
Experimental setup
for flexural testing
and tested 3D printed
component

modulus and glass transition temperature, whereas HIPS was observed just opposite of PLA (Table I). The multi-material printing of ABS, PLA and HIPS were performed and then thermal and mechanical properties have been analysed to optimize the set of input process variables.

4.1 Thermal characteristics

Figure 11 shows the comparative DSC based thermo graphs of ABS, PLA and HIPS thermoplastic material for glass transition temperature and integral heat energy during heating as well as cooling. DSC curves resulted in the interesting fact that ABS, PLA and HIPS are compatible to each other as all are having the similar ranges of integral heat integral value. It was observed that integral heat intake during heating of ABS has taken 13.63 mJ energy, PLA taken 14.71 mJ energy and HIPS has taken 11.71 mJ. This interesting fact reveals that multi-material can give the better layer connectivity by 3DP if those are having the similar ranges of heat capacities. On the other hand, during solidification of the material it was observed that ABS released 13.52 mJ, PLA released 10.80 mJ, whereas HIPS released 10.87 mJ energy those are also similar.

4.2 Tensile properties

Break elongation, percentage elongation at break, break load, break strength and Young’s modulus have been observed as an output by varying input processing variables, such as material combination, infill percentage and printing speed (Table II). The break elongation of ABS was observed as 4.94 mm, for PLA, it was 5.3 mm and minimum for HIPS 2.47 mm. Break elongation was desired as ‘smaller is better’ and it was observed that for experiment number 1 the break elongation was observed as 2.85mm which was larger than HIPS but at the same time it was smaller than ABS and PLA. So, this observation resulted into the positive outcome that multi-material printing

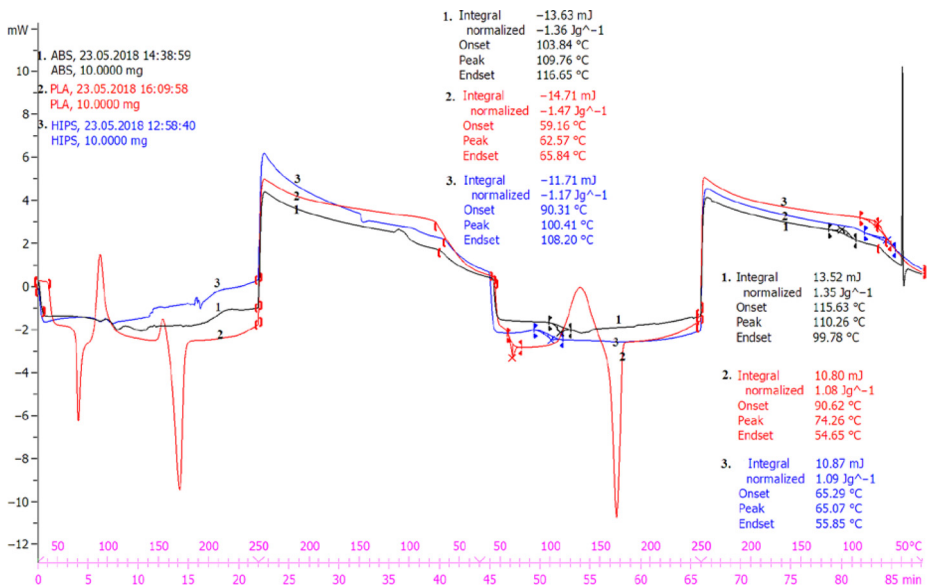


Figure 11. DSC curves of ABS, PLA and HIPS

with HIPS polymer can reduce the elongation behaviour of composite material. Similar observations were resulted for percentage elongation at break as in case of experiment number 1, where percentage elongation was larger than HIPS but significant smaller than ABS and PLA. The break load property is one of the most important properties for selection of engineering components. The break load of PLA (254.1 N) was observed larger than ABS (188.3 N) and HIPS (72.72 N). For experiment number 3, break load was observed as 186.21 N which is little smaller than PLA and ABS but largely greater than HIPS. Similarly break strength of PLA (13.24 MPa) and ABS (9.7 MPa) was largely greater than HIPS (3.79 MPa), but combined printing of all these material at experiment number 3 (9.7) was equal to ABS and significant smaller than PLA but largely greater than HIPS. The most interesting results were observed in the case of Young's modulus where it was having Young's modulus of PLA 47.9 MPa, ABS of 175 MPa and for HIPS 112.5 MPa. Printing at experiment number 4 resulted in the Young's modulus of 325 MPa having higher value than all of the single materials. Figure 12 shows the comparative graphs of break elongation, percentage elongation at break, break load, break strength and Young's modulus with respect of varying input process parameters and virgin materials.

Figure 13 shows the stress versus strain curves for 3D printed multi-material components at all experiment conditions including virgin's samples of ABS, PLA and HIPS. Here, it is clear that virgin HIPS material observed in minimum value of tensile strength and elongations. Similarly, virgin PLA was achieved maximum values of strength of tensile strength and elongation properties. As the practical application requires the requirement for maximum strength with minimum elongation, HIPS was having most desired elongation and PLA was having most desired tensile strength values. After 3D printing of multi-material component, it was observed that tensile strength and elongation values of all multi-material printed components were observed intermediate to the HIPS and ABS which shows the usefulness of present study.

4.3 Pull out test

Pull out testing of 3D printed multi-material component resulted in observations of break elongation, percentage elongation at break, break load and break strength with varying the input process variables such as; material combination, infill percentage and printing speed. Elongation properties were desired 'smaller is better', whereas break load and break strength were desired 'larger is better'. Break elongation and percentage elongation at break at experiment number 9 (3.8 mm and 2 per cent) was observed most desired lesser than all single materials. Break load of ABS was 116.55 Kg, PLA was 156.34 Kg and HIPS of 87.84 Kg, multi-material component at experiment no. six resulted in 92.24 Kg which was smaller value than ABS and PLA but greater than HIPS. Similar results were observed for the break strength where at experiment number 6, the break strength was smaller than ABS and PLA but greater than HIPS. Figure 14 shows the results of pull out properties of single as well as 3D printed multi-material components.

Figure 15 shows the comparative curves of stress versus strain of 3D printed multi-material components. From here, it was noted that strength of the most of the multi-material component were come under ranges below PLA and ABS and above than HIPS.

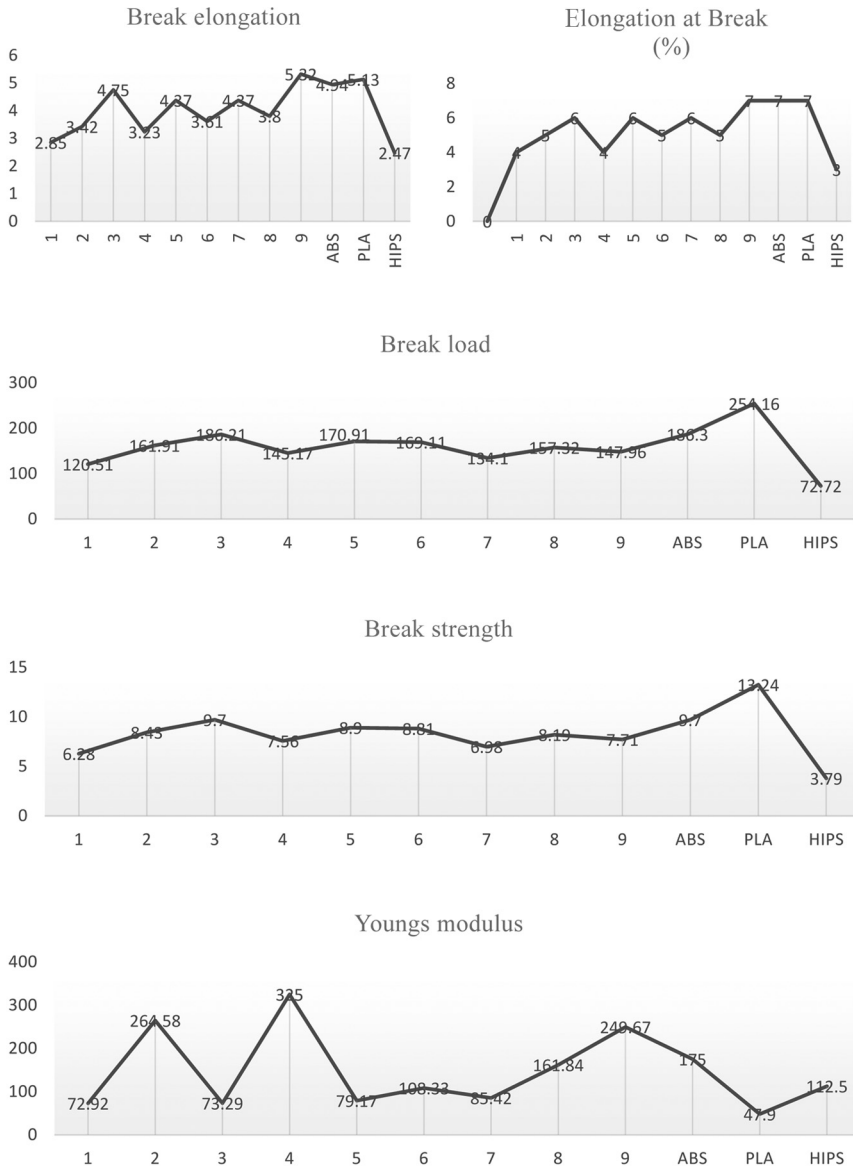


Figure 12.
Tensile properties of
3D printed multi-
material component

4.4 Micrographic observations

Photo-micrographic observations have been made at 30X magnification with Tool maker's microscope. The eye piece of tool maker microscope was configured with 15X magnification whereas object lance with 2X, so there was total of 30X magnification. It was observed that PLA resulted in the maximum value of break strength because their layers are fused well

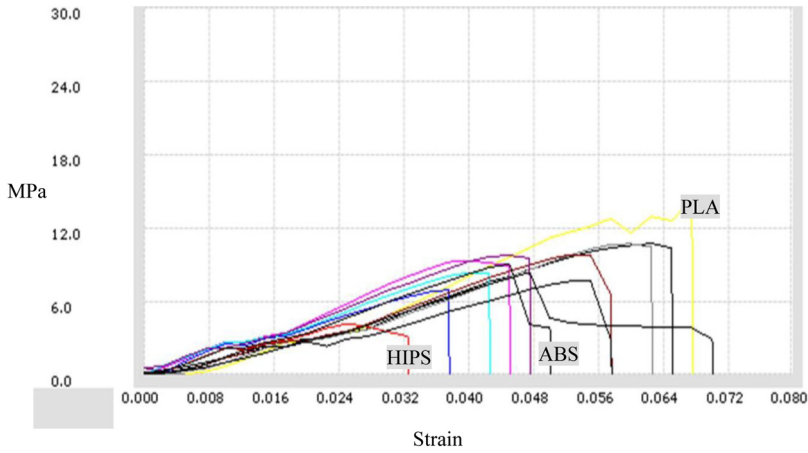


Figure 13. Stress Vs. strain curves for multilateral component in tensile testing

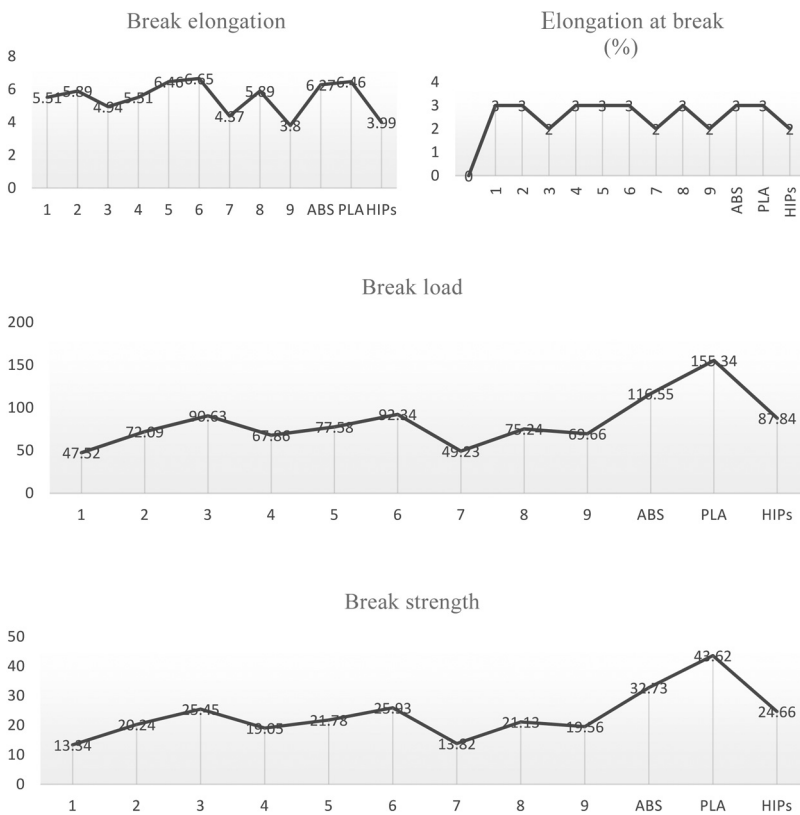
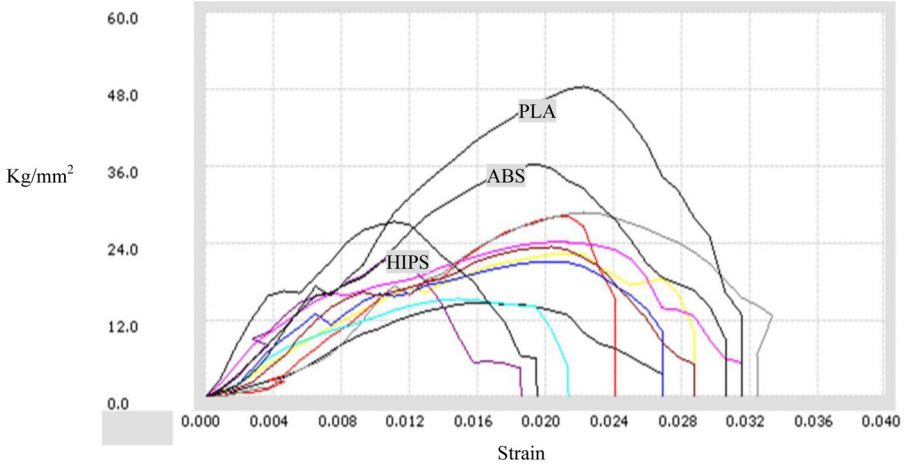


Figure 14. Pull out properties of 3D printed single and multi-material printed components

Figure 15.
Stress vs. strain
curves for 3D printed
multi-material
component in pull out
test



resulting in more uniformity. The tensile strength for experiment number 3 (Table II) was observed as maximum, the interlayer connectivity of ABS, PLA and HIPS thermoplastic was observed as better (Figure 16). For experiment number 1, where tensile strength was resulted in the minimum values the micrographs highlights that the layer connectivity in this case in not uniform so less strength was attained (Figure 16).

4.5 Optimization of input process variables

For the production purpose at large scale of 3DP multi-material component, it is necessary to have the optimized set of input process variable. The optimization of input process variables based on the tensile and pull out outcomes have been conducted to determine the optimized set of input process variables.

Towards optimizing input process variable for selection of best contributing process parameters, the variance over Signal to noise (SN) have been calculated. SN ratio is always desired to be maximum, conversion of material properties to SN ratio is predicted either “Smaller is better” or “Larger is better”. For Mechanical properties, such as break load, break strength and Young’s modulus, it is always to be maximum, whereas for break elongation and percentage elongation at break it was desired to be minimum. For properties which desired larger is better, SN ratios can be calculated as:

$$\eta = -10 \log \left[\frac{1}{n} \sum_{k=1}^n \frac{1}{y^2} \right] \quad (2)$$

For properties which desired Smaller is better, SN ratios can be calculated as:

$$\eta = -10 \log \left[\frac{1}{n} \sum_{k=1}^n y^2 \right] \quad (3)$$

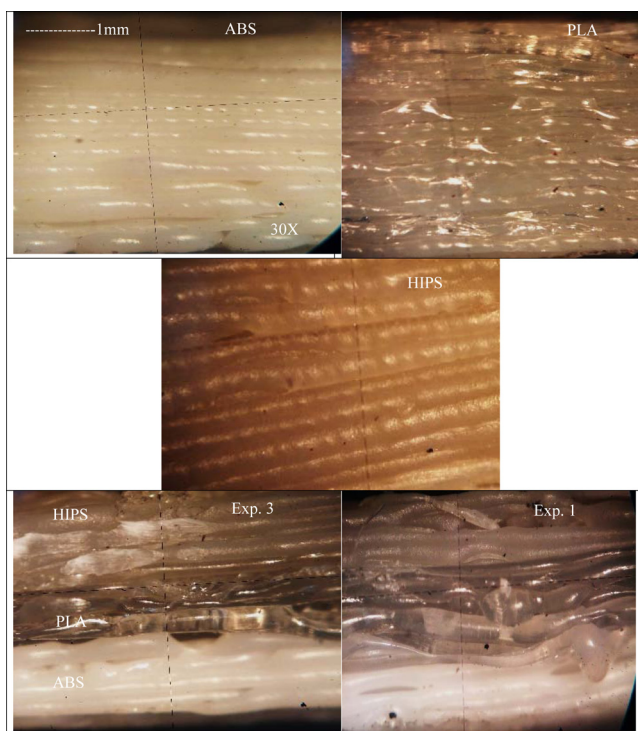


Figure 16.
Micrographs of ABS,
PLA, HIPS and multi-
material components

Where η is SN ratio, n is the number of experiment and y is the material properties at experiment number k .

Figure 17 shows linear model graph for SN ratios of tensile properties with respect to input process variables. From here, it is noted that break elongation and percentage elongation at break was resulted in the better SN ration because of APH material combination, 60 infill density and 50mm/sec printing speed. For break load and break strength, material combination of PHA, 100 per cent infill percentage and 70 mm/sec printing speed came as the best setting. For Young's modulus material combination as HAP, 80 per cent infill density and 60 mm/sec printing speed resulted in the best setting of process parameters.

Observations from pull out testing categorised as: break elongation and percentage elongation at break in 'smaller is better', whereas break load and break strength in 'larger is better'. Figure 18 shows the linear model graph for SN ratios of pull out properties. It should be noted that for break elongation and percentage elongation at break material combination HAP, 100 per cent infill percentage and 60 mm/sec printing speed resulted in the factors which contributed largely for SN ratio so it was best set of parameters. For break load and break strength, material combination of PHA, 100 per cent infill density and 70 mm/sec printing speed observed as the best set of input process variables.

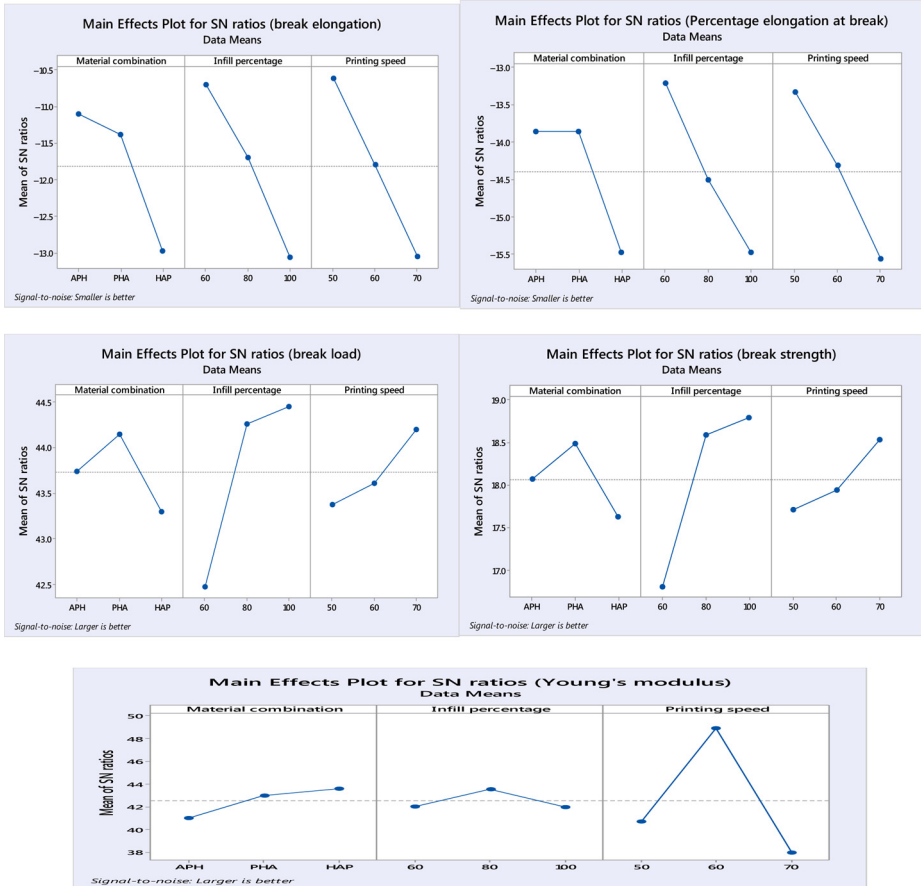


Figure 17.
Linear model for SN ratios of tensile properties

From here, it was observed that for changes in the break elongation as tensile properties of 3DP multi-material component, material combination contributed 25.41 per cent, infill percentage contributed 35.31 per cent and printing speed was contributed maximum as 37.0 per cent. The residual error was observed 2.25 per cent that shows the good control over the processing of components (Table III).

Table IV shows the response table for SN ratio of break elongation as the key for ranking of input process variables. The printing speed was ranked as 1, infill percentage as Rank 3 and material combination was ranked 1 based on changes in SN ratios.

Now the use of statistical formula predicted the value of break elongation at optimized set of process variable as suggested in Figure 18.

The optimum value of break elongation as tensile properties can be predicted by using following equation:

$$\eta_{opt} = m + (m_{A1} - m) + (m_{B1} - m) + (m_{C1} - m) \tag{4}$$

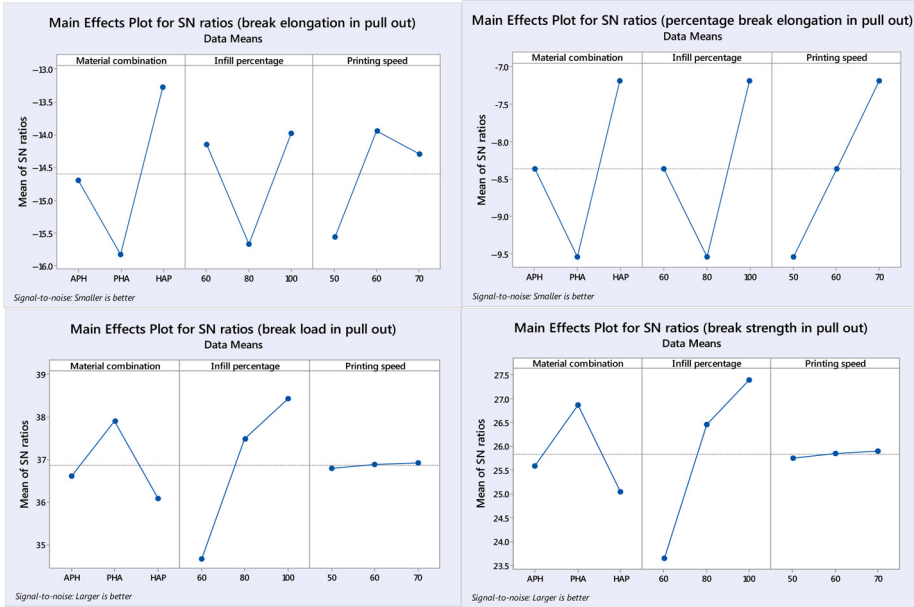


Figure 18. Linear model for SN ratios of pull out properties

Source	DF	Seq SS	Adj SS	Adj MS	F	P	% age contribution
Material combination	2	6.1151	6.1151	3.0576	11.30	0.081	25.41
Infill Percentage	2	8.4992	8.4992	4.2496	15.70	0.060	35.31
Printing Speed	2	8.9100	8.9100	4.4550	16.46	0.057	37.02
Residual Error	2	0.5414	0.5414	0.2707			2.25
Total	8	24.0656					

Table III. Analysis of variance for SN ratios of break elongation in tensile loading

Level	Material combination	Infill percentage	Printing speed
1	-11.10	-10.70	-10.61
2	-11.38	-11.70	-11.79
3	-12.97	-13.07	-13.05
Delta	1.87	2.37	2.44
Rank	3	2	1

Table IV. Response table for signal to noise ratios (smaller is better)

Where 'm' is the overall mean of SN ratio, m_{A_1} is the mean of SN ratio for material combination at Level 1, m_{B_1} is the mean of SN ratio for infill percentage at Level 1 and m_{C_1} is the mean of SN data for printing speed at Level 1.

$y_{opt}^2 = (1/10)^{\eta_{opt}/10}$ for properties, smaller is better; and $y_{opt}^2 = (10)^{\eta_{opt}/10}$ for properties, larger is better.

Considering break elongation as smaller is better:

$$y_{\text{opt}}^2 = (1/10)^{\eta_{\text{opt}}/10} \quad (5)$$

Calculation:

Overall mean of SN ratios (m) for peak load was calculated as:

$m = -11.81\text{dB}$ (By calculating SN ratios at particular experimental condition)

Now from response table of signal to noise ratio, $m_{A1} = -11.10$, $m_{B1} = -10.70$, $m_{C1} = -10.61$ (From [Table IV](#))

Now from [Equation \(4\)](#):

$$\eta_{\text{opt}} = -11.81 + (-11.10 + 11.81) + (-10.70 + 11.81) + (-10.61 + 11.81)$$

$$\eta_{\text{opt}} = -8.79$$

Now, from [Equation \(5\)](#):

$$y_{\text{opt}}^2 = (1/10)^{\eta_{\text{opt}}/10}$$

$$y_{\text{opt}}^2 = (1/10)^{-8.79/10}$$

$$y_{\text{opt}} = 2.75 \text{ mm}$$

The predicted optimum value for break elongation in tensile testing = 2.75 mm.

Similarly, the remaining properties in tensile as well as pull out testing have been predicted and shown in [Table V](#).

4.6 Combined optimization of input process variables

There are number of setting which have been predicted for each of the properties and those are available in the various combinations. For the actual production purpose, it must have the one single parametric setting so that no requirement to change the hardware/software of the machine. So keeping this prospect all the input parameter in a single setting has been determined by combining SN ratios. After combining the SN ratios of all the tensile and pull out properties, there was a single parametric setting, that is, APH material combination, 100 per cent infill density and 60mm/sec has been achieved ([Figure 19](#)).

4.7 Properties at optimized settings

As predicted that APH material combination, 100 per cent infill percentage and 60 mm/sec printing speed was calculated as optimized set of input process parameters for production prospects. At optimized set of process parameters printing of standard components have been prepared and then properties like flexural strength, thermal conductivities have been investigated.

4.7.1 Flexural strength at break. At predicted set of input process variables, the flexural test of 3D printed multi-material component has been checked which is shown in [Figure 20](#). It was observed that flexural strength of HIPS was noted minimum as 2.01 MPa and PLA was noted maximum as 9.07 MPa, whereas ABS was having 7.04 MPa. Printing of these materials at predicted setting resulted in an interesting fact that flexural strength was attained higher than HIPS material as 2.96 MPa but lower than PLA and ABS.

4.7.2 Thermal conductivities. [Figure 21](#) shows the thermal conductivity plot for 3D printed component of single as well as multi-material component. It was noted that PLA was

Output	Attribute	Sub-output parameters				
		Break elongation	% elongation at Break	Break load	Break strength	Youngs modulus
Tensile properties	$\eta_{opt}(dB)$	-8.79	-11.71	45.37	19.69	50.98
	Predicted value (V_{opt})	2.75 mm	3.85 %	185.7N	9.65 MPa	353.99MPa
Pull out properties	Best settings for predicted value	Material combination- APH, Infill percentage -60%, Printing speed-50mm/sec	Material combination- APH, Infill percentage -60%, Printing speed-50mm/sec	Material combination- PHA, Infill percentage -100%, Printing speed-70mm/sec	Material combination- PHA, Infill percentage -100%, Printing speed-70mm/sec	Material combination- HAP, Infill percentage -80%, Printing speed-60mm/sec
	Actual value at optimized setup	Material combination- HAP, Infill percentage -100%, Printing speed-60mm/sec	Material combination- HAP, Infill percentage -100%, Printing speed-70mm/sec	Material combination- PHA, Infill percentage -100%, Printing speed-70mm/sec	Material combination- PHA, Infill percentage -100%, Printing speed-70mm/sec	Material combination- PHA, Infill percentage -100%, Printing speed-70mm/sec

Table V.
Calculated/predicted
mechanical
properties and
experimentally
determined values

Figure 19.
Predicted set of input
process variable for
production

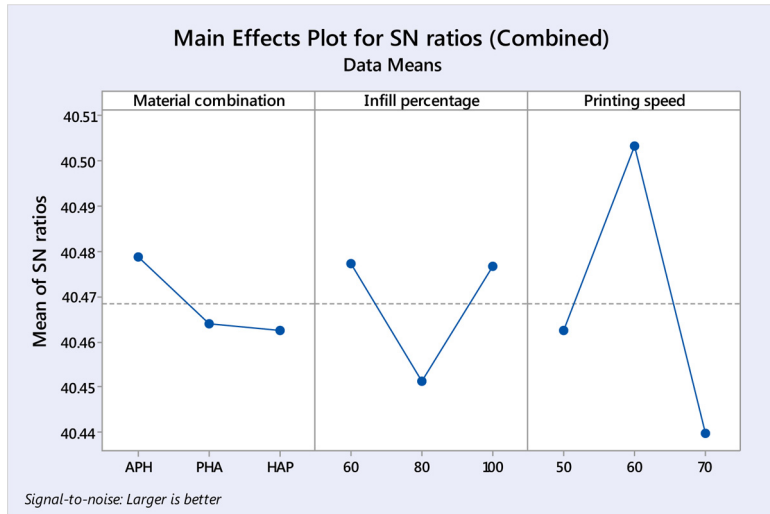


Figure 20.
Flexural strength of
3D printed
component at
predicted setting

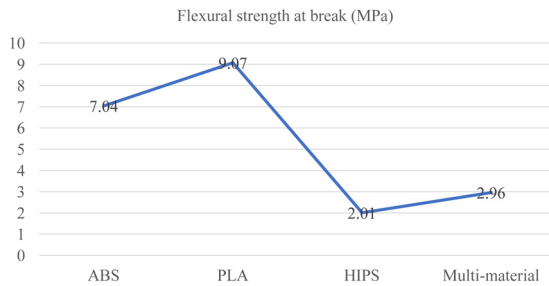
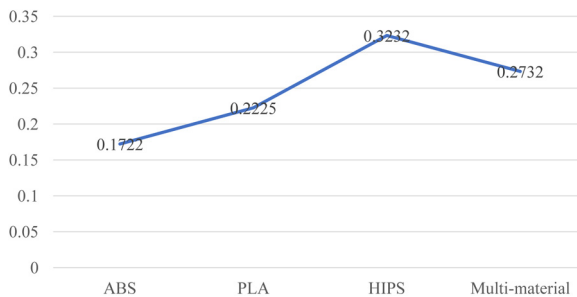


Figure 21.
Thermal conductivity
of 3D printed
component at
predicted setting



having thermal conductivity of 0.2225 W/m.K, ABS of 0.1722W/m.K and HIPS of 0.3232W/m.K. For structural applications, it requires the thermal conductivity to be desired minimum. Multi-material printing of these material resulted in thermal conductivity of 0.2732W/m.K ($dt/dT = 0.814$ K/s) which was lesser than HIPS material shows the utility of multi-material 3D printing.

5. Conclusions

Following conclusions have been made from present study of 3DP for recycled ABS, PLA and HIIPS thermoplastic materials:

- Tensile testing of 3D printed multilateral component resulted in an interesting observation. It was noted that Young's modulus of multi-material component (325 MPa) was observed higher at experiment number 3, than single thermoplastic (Young's modulus of PLA 47.9 MPa, ABS of 175 MPa and for HIPS 112.5 MPa).
- Pull out testing have revealed the fact that elongation and strength properties of 3DP can be controlled through multi-material printing at predicted input processing setting. It was noted that break elongation of multi-material component was observed smaller as compared to ABS and PLA. At the same time, break load and break strength has been observed greater than HIPS in case of pull out tests.
- 3DP of multi-material component at predicted setting resulted in an interesting fact that flexural strength was attained higher than HIPS (2.01 MPa) material as 2.96 MPa but lower than PLA (9.07 MPa) and ABS (7.04 MPa).
- It was noted that PLA was having thermal conductivity of 0.2225 W/m.K, ABS of 0.1722W/m.K and HIPS of 0.3232W/m.K. For structural applications, it requires the thermal conductivity to be desired minimum. Multi-material printing of these material resulted in thermal conductivity of 0.2732W/m.K ($dt/dT = 0.814$ K/s) which was lesser than HIPS material shows the utility of multi-material 3DP.

References

- Bandyopadhyay, A. and Heer, B. (2018), "Additive manufacturing of multi-material structures", *Materials Science and Engineering: R: Reports*, Vol. 129, pp. 1-16.
- Barretta, R., Feo, L., Luciano, R., Marotti de Sciarra, F. and Penna, R. (2017), "Nano-beams under torsion: a stress-driven nonlocal approach", *PSU Research Review*, Vol. 1 No. 2, pp. 164-169.
- Bittner, S.M., Guo, J.L., Melchiorri, A. and Mikos, A.G. (2018), "Three-dimensional printing of multilayered tissue engineering scaffolds", *Materials Today*, doi: <https://doi.org/10.1016/j.mattod.2018.02.006>.
- Guessasma, S., Nouri, H. and Roger, F. (2017), "Microstructural and mechanical implications of microscaled assembly in droplet-based multi-material additive manufacturing", *Polymers*, Vol. 9 No. 12, p. 372.
- Hambali, R.H., Cheong, K.M. and Azizan, N. (2017), "Analysis of the influence of chemical treatment to the strength and surface roughness of FDM", *Iop Conference Series: Materials Science and Engineering*, Vol. 210, p. 012063.
- Kariz, M., Sernek, M., Obućina, M. and Kuzman, M.K. (2018), "Effect of wood content in FDM filament on properties of 3D printed parts", *Materials Today Communications*, Vol. 14, pp. 135-140.
- Kumar, R. and Singh, R. (2018), "Prospect of graphene for use as sensors in miniaturized and biomedical sensing devices", In: Saleem H. (editor-in-chief), *Reference Module in Materials Science and Materials Engineering*, Elsevier, Oxford. pp. 1-13.
- Kumar, R., Singh, R., Ahuja, I.P.S., Amendola, A. and Penna, R. (2018), "Friction welding for the manufacturing of PA6 and ABS structures reinforced with Fe particles", *Composites Part B: Engineering*, Vol. 132, pp. 244-257.
- Kumar, R., Singh, R., Ahuja, I.P.S., Penna, R. and Feo, L. (2017a), "Weldability of thermoplastic materials for friction stir welding-A state of art review and future applications", *Composites Part B: Engineering*, Vol. 137, pp. 1-15.
- Kumar, R., Singh, R., Hui, D., Feo, L. and Fraternali, F. (2017b), "Graphene as biomedical sensing element: State of art review and potential engineering applications", *Composites Part B: Engineering*, Vol. 134, pp. 193-206.

- Lee, J.Y., An, J. and Chua, C.K. (2017), "Fundamentals and applications of 3D printing for novel materials", *Applied Materials Today*, Vol. 7, pp. 120-133.
- Ma, R.R., Belter, J.T. and Dollar, A.M. (2015), "Hybrid deposition manufacturing: Design strategies for multimaterial mechanisms via three-dimensional printing and material deposition", *Journal of Mechanisms and Robotics*, Vol. 7 No. 2, p. 021002.
- Martin, O. and Averous, L. (2001), "Poly (lactic acid): plasticization and properties of biodegradable multiphase systems", *Polymer*, Vol. 42 No. 14, pp. 6209-6219.
- Meisel, N.A. (2015), "Design for additive manufacturing considerations for self-actuating compliant mechanisms created via multi-material PolyJet 3D printing", Doctoral dissertation, Virginia Polytechnic Institute and State University. 1-272.
- Mohammed, M., Tatini, J., Cadd, B., Peart, P. and Gibson, I. (2016), "Applications of 3D topography scanning and multi-material additive manufacturing for facial prosthesis development and production", in *Proceedings of the 27th Annual International Solid Freeform Fabrication Symposium*, pp. 1695-1707.
- Momeni, F., Liu, X. and Ni, J. (2017), "A review of 4D printing", *Materials and Design*, Vol. 122, pp. 42-79.
- Muguruza, A., Bo, J.B., Gómez, A., Minguella-Canela, J., Fernandes, J., Ramos, F. and Cirera, A. (2017), "Development of a multi-material additive manufacturing process for electronic devices", *Procedia Manufacturing*, Vol. 13, pp. 746-753.
- Ngo, T.D., Kashani, A., Imbalzano, G., Nguyen, K.T. and Hui, D. (2018), "Additive manufacturing (3D printing): a review of materials, methods, applications and challenges", *Composites Part B: Engineering*, doi: [10.1016/j.compositesb.2018.02.012](https://doi.org/10.1016/j.compositesb.2018.02.012).
- Rutkowski, J.V. and Levin, B.C. (1986), "Acrylonitrile-butadiene-styrene copolymers (ABS): pyrolysis and combustion products and their toxicity – a review of the literature", *Fire and Materials*, Vol. 10 Nos 3-4, pp. 93-105.
- Singh, R., Fraternali, F., Bonazzi, G. and Hashmi, M.S.J. (2018a), "Kumar R. and ranjan N, investigations for development of feed stock filament of fused deposition modeling from recycled polyamide", In: Saleem H. (editor-in-chief), *Reference Module in Materials Science and Materials Engineering*, Elsevier, Oxford, pp. 1-20.
- Singh, R. and Kumar, R. (2017), "Development of Low-Cost Graphene-Polymer blended in-House Filament for fused deposition modeling", In: Saleem H. (editor-in-chief), *Reference Module in Materials Science and Materials Engineering*, Elsevier, Oxford, pp. 1-10.
- Singh, R., Kumar, R. and Ahuja, I.P.S. (2017b), "Thermal analysis for joining of dissimilar polymeric materials through friction stir welding", In: Saleem H. (editor-in-chief), *Reference Module in Materials Science and Materials Engineering*, Elsevier, Oxford, pp. 1-13.
- Singh, R., Kumar, R., Feo, L. and Fraternali, F. (2016), "Friction welding of dissimilar plastic/polymer materials with metal powder reinforcement for engineering applications", *Composites Part B: Engineering*, Vol. 101, pp. 77-86.
- Singh, R., Kumar, R. and Hashmi, M.S.J. (2017c), "Friction welding of dissimilar Plastic-Based material by MetalPowder reinforcement", In: Saleem H., *Reference Module in Materials Science and Materials Engineering*, Elsevier, Oxford, Vol. 13, pp. 1-16.
- Singh, R., Kumar, R. and Kumar, S. (2017d), "Polymer waste as fused deposition modeling feed stock filament for industrial applications", In: Saleem H. (editor-in-chief), *Reference Module in Materials Science and Materials Engineering*, Elsevier, Oxford, pp. 1-12.
- Singh, R., Kumar, R., Mascolo, I. and Modano, M. (2018b), "On the applicability of composite PA6-TiO2 filaments for the rapid prototyping of innovative materials and structures", *Composites Part B: Engineering*, Vol. 143, pp. 132-140.
- Singh, R., Kumar, R. and Ranjan, N. (2018c), "Sustainability of recycled ABS and PA6 by banana fiber reinforcement: Thermal, mechanical and morphological properties", *Journal of the Institution of Engineers (India): Series C*, pp. 1-10, doi: [10.1007/s40032-017-0435-1](https://doi.org/10.1007/s40032-017-0435-1).

-
- Singh, R., Kumar, R., Ranjan, N., Penna, R. and Fraternali, F. (2018d), "On the recyclability of polyamide for sustainable composite structures in civil engineering", *Composite Structures*, Vol. 184, pp. 704-713.
- Singh, S. and Singh, R. (2016), "Experimental investigations for use of nylon6 industrial waste as FDM feedstock filament for investment casting applications", *Indian Journal of Engineering and Material Sciences (IJEMS)*, Vol. 23, pp. 181-187.
- Vu, I.Q., Bass, L.B., Williams, C.B. and Dillard, D.A. (2018), "Characterizing the effect of print orientation on interface integrity of multi-material jetting additive manufacturing", *Additive Manufacturing*, Vol. 22, pp. 447-461, doi: <https://doi.org/10.1016/j.addma.2018.05.036>.

Corresponding author

Ilenia Farina can be contacted at: ilenia.farina@uniparthenope.it

For instructions on how to order reprints of this article, please visit our website:

www.emeraldgrouppublishing.com/licensing/reprints.htm

Or contact us for further details: permissions@emeraldinsight.com